Published: 29 March 2022

RESEARCH-ARTICLE

Ultra Low-Latency Backscatter for Fast-Moving Location Tracking

JINGXIAN WANG, Carnegie Mellon University, Pittsburgh, PA, United States

VAISHNAVI RANGANATHAN, Microsoft Research, Redmond, WA, United States

JONATHAN LESTER, Microsoft Research, Redmond, WA, United States

SWARUN KUMAR, Carnegie Mellon University, Pittsburgh, PA, United States

Open Access Support provided by:

Microsoft Research

Carnegie Mellon University

Ultra Low-Latency Backscatter for Fast-Moving Location Tracking

JINGXIAN WANG, Carnegie Mellon University
VAISHNAVI RANGANATHAN, Microsoft Research, Redmond
JONATHAN LESTER, Microsoft Research, Redmond
SWARUN KUMAR, Carnegie Mellon University

This paper explores building an ultra-low latency and high-accuracy location tracking solution using battery-free tags. While there is rich prior work on location tracking with battery-free RFID tags and backscatter devices, these systems typically face tradeoffs with accuracy, power consumption, and latency. Such limitations make these existing solutions unsuitable for emerging applications like industrial augmented reality which requires tracking fast-moving machinery; monitoring indoor sports activities that require real-time tracking of fast-moving objects with high precision and under stringent latency constraints.

We propose and demonstrate FastLoc, a precision tracking system that locates tiny, battery-free analog backscatter tags at sub-millisecond latency and sub-centimeter accuracy. FastLoc is a hybrid system that simultaneously uses RF and optical signals to track tiny tags that can be attached to everyday objects. FastLoc leverages the RF channel responses from tags for estimating the coarse region where the tags may be located. It *simultaneously* uses the sensed optical information modulated on the backscatter signals to enable fine-grained location estimation within the coarse region. To achieve this, we design and fabricate a custom analog tag that consumes less than 150 *uW* and instantaneously converts incident optical signals to one-shot wideband harmonic RF responses at nanosecond latency. We then develop a static high-density distributed-frequency structured light pattern that can localize tags in the area of interest at a sub-centimeter accuracy and microsecond-scale latency. A detailed experimental evaluation of FastLoc shows a median accuracy of 0.7 cm in tag localization with a 0.51 ms effective localization latency.

CCS Concepts: • **Human-centered computing** → **Ubiquitous and mobile computing**; • **Hardware** → *Wireless devices.*

ACM Reference Format:
Jingxian Wang, Vaishnavi Ranganathan, Jonathan Lester, and Swarun Kumar. 2022. Ultra Low-Latency Backscatter for Fast-Moving Location Tracking. *Proc. ACM Interact. Mob. Wearable Ubiquitous Technol.* 6, 1, Article 30 (March 2022), 22 pages. https://doi.org/10.1145/3517242

1 INTRODUCTION

This paper asks: "Can we achieve location tracking with battery-free tags at *sub-millisecond* latency and sub-centimeter accuracy using low-cost infrastructure?" While the rich literature on battery-free localization systems using RF tags [18, 28, 30, 61] traditionally make accuracy the prime metric of performance, this paper also focuses on a different yet crucial metric: *latency*. Ultra-low latency is critical to emerging applications such as industrial augmented reality and indoor sports activities tracking. Consider for example, tracking tag mounted motor parts spinning at speeds of up to 45 km/h (2500 rpm), where even 32 milliseconds of latency (e.g. of the commercial optical tracking system – Lighthouse [11] used by SteamVR and HTC Vive) misses 40 cm of movement.

Authors' addresses: Jingxian Wang, Carnegie Mellon University, jingxian@cmu.edu; Vaishnavi Ranganathan, Microsoft Research, Redmond, Vaishnavi.Ranganathan@microsoft.com; Jonathan Lester, Microsoft Research, Redmond, jonathan.lester@microsoft.com; Swarun Kumar, Carnegie Mellon University, swarun@cmu.edu.

2474-9567/2022/3-ART30
https://doi.org/10.1145/3517242

Localization and tracking research based on RF signals has a broad range that spans from only using RF signal properties to augmenting those signals with other legacy localization methods which use acoustics or visible light to achieve centimeter-level accuracy [19, 27, 39]. A review of such work in [62] highlights the key tradeoffs these systems make between energy efficiency, complexity, accuracy and latency. State-of-the-art localization systems with sub-centimeter accuracy, in both optical and RF-based systems, force a choice between latency and complexity of the infrastructure and tags. Traditional active optical and IMU based [12, 20] AR tags tend to be bulky and require batteries. Further, commercial optical motion capture systems that support passive retro-reflective markers for tracking require multiple high-resolution cameras which are too expensive and difficult to set up [17] or using time-intensive mechanical laser scans [11]. Similarly, more recent RF-based localization solutions for battery-free tags either require time-consuming scans over multiple frequencies to emulate a wide bandwidth (~6.4 seconds [30]), or require multiple coordinated transmitters [28, 61]. Ideally, we seek a system that is simultaneously low-cost, ultra low-latency and millimeter-accurate to localize passive tags.

We present FastLoc, a novel backscatter-based localization system which: 1) enables sub-millisecond latency and sub-centimeter accuracy real-time object tracking; 2) uses low-cost infrastructure that consists of a single-tone RF transmitter and a pair of low-cost optical projectors; 3) designs custom battery-free, simple analog and cross-technology FastLoc tags that sense optical signals and communicate them as an instantaneous wide-band RF response at nanoseconds latency (see Fig. 1 a); 4) develops an intelligent projected optical pattern for sub-centimeter localization; 5) enables easy tracking of multiple tags simultaneously at low-latency. We show how our ultra-low power custom tag design achieves the best of both RF and optical systems – achieving 0.7 cm accuracy and 0.51 ms scanning latency in line-of-sight, validated through extensive experimental evaluation. Even with only the RF signals, FastLoc achieves a fast and coarse non-line-of-sight (NLOS) accuracy of 31 cm on average, which is further enhanced by the optical augmentation for fine line-of-sight (LOS) tracking. In addition, FastLoc tags are designed to operate at less than 150 uW, and can operate with energy harvested from the RF signal.

The key idea behind FastLoc is to design a one-shot optical projector pattern that elicits an instantaneous RF response from the tag to identify its location. FastLoc's tags are designed to modulate on top of radio signals from an always-on sub-GHz RF reader, only when illuminated by light at specific frequencies. When the optical sensor on the FastLoc tags are illuminated by the projected pattern, each tag modulates the optical information as an inherently *wide-band* RF response that is captured by the nearby RF reader at ultra low-latency. FastLoc then uses this wide-band channel response to estimate a coarse region where the tag may be located (decimeter wide). FastLoc then uses the color of incident light at the tag that is directly reported in its modulated RF response to further refine localization. This is because FastLoc leverages a novel structured spatial pattern of colored light from the projector that always illuminates pixels within the coarse tag region with different colors. We show how this method further refines tag localization to sub-centimeter accuracy. The rest of this paper addresses two key challenges in FastLoc's architecture (see Fig. 1 b): the design of the one-shot wide-band RF response from the tag and the optical pattern from the projector .

Designing the RF Tag Response: Our first objective in designing the tag response is to ensure that it can be located within as small a region as possible with a single query (shortest time). Indeed, the rich prior work on locating battery-free tags informs us that the key metric of interest that dictates location resolution is the tag response bandwidth. Unfortunately, the state-of-the-art approach of hopping across frequencies to stitch together high (virtual) bandwidth goes against our low-latency objective, since such hopping can take hundreds of milliseconds and even seconds.

To address this challenge, FastLoc achieves a one-shot wideband channel estimation of the tag by only sending a single-tone RF signal from one nearby transmitter. FastLoc's secret sauce is a novel design of a backscatter tag that generates a series of harmonics across a wide bandwidth. Typically, such harmonics are naturally generated by analog circuitry during the RF backscatter process but are normally filtered out as undesirable spurious

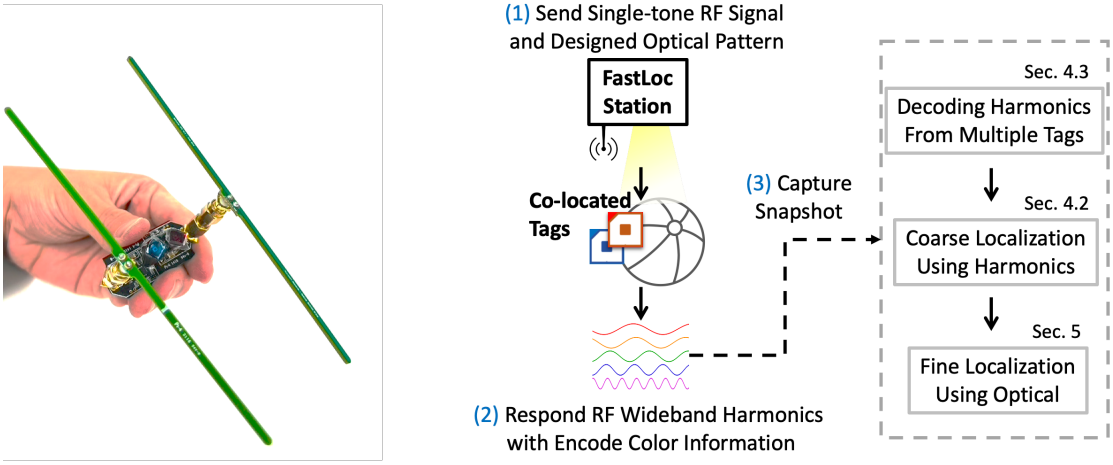

(a). Battery-free FastLoc Tag Setup

(b). FastLoc's Architecture

Fig. 1. (a) Prototype device: A single FastLoc tag contains a photodiode and a simple analog RF-backscatter design. We use two co-located tags to localize, as shown. (b) Architecture: FastLoc uses a pair of blue-filtered and red-filtered co-located FastLoc tags, with combined optical and RF capability, to localize the tagged object. (See detailed description in Sec. 3.1.)

out-of-band transmissions. In contrast, FastLoc embraces these harmonics to improve tag response bandwidth and therefore localization accuracy. From our experiments, the harmonics from one FastLoc tag can expand as much as 50 MHz bandwidth. By leveraging one-shot wideband harmonic response at the reader, FastLoc applies a super-resolution MUSIC algorithm to localize the tags. FastLoc further supports simultaneously decoding multiple such tags even when the harmonic signals from different tags collide with each other. At the end of this process, FastLoc estimates a coarse location of each tag based on the wideband harmonic responses, which can be further refined to sub-centimeter accuracy through the optical response reported by the tags. Sec. 4 further details our approach to the RF-based coarse localization.

Designing the Optical Projector Pattern: Following the coarse localization, FastLoc performs a fine-grained localization of its tags within the coarse region where the tag(s) have already been identified based on their RF responses. Traditionally, virtual reality scanning systems address searches of this nature by using multiple line lasers that are mechanically steered over the space of interest, but are subject to steering latency.

In contrast, FastLoc builds on top of low-cost commercial optical projectors to project a specially designed spatial light pattern (i.e. of differently colored pixels) over the entire space. FastLoc's optical pattern is specifically engineered to ensure that even adjacent pixels – about a few mm-wide, when projected – can be disambiguated based on the light color that a tag senses. Yet, to ensure low cost and power of the tag, this design constraint quickly exhausts the number of distinct colors that can be projected. To remedy this, FastLoc spatially replicates and interleaves these colors intelligently so that no two pixels within the same coarse RF region will map to the same color, *without* knowing a priori where this coarse region is located. This allows FastLoc to apply a single, static projector pattern to simultaneously locate multiple tags in a one-shot, regardless of where they are located in the area of interest, at sub-centimeter accuracy. Sec. 5 describes our design of the optical projected pattern.

Applications: FastLoc opens up several applications which we briefly explain below and evaluate in Sec. 7.6:

- Motion Tracking for Robotic Manufacturing: FastLoc locates the fast-moving nozzle inside the laser cutter with ultra-low latency and high precision. Such applications are useful for real-time tracking of fast robotic arms in places like vehicle assembly lines and warehouses.
- Predictive Maintenance: FastLoc can track fast-moving machinery and detect mechanical failure and displacement at the first sign of trouble with ultra-low latency. We show that FastLoc tracks the fine-grained trajectory of a spinning motor part at high precision.
- Fine-grained Gesture Sensing for E-sports and VR Games: FastLoc can detect the fine-grained gestures of human body when users play games. Such a system would be useful especially for head-mounted Ego AR applications to enable locating and interacting with tagged objects. For example, we show that FastLoc transforms an ordinary ping-pong racket to be a VR interaction tool by attaching our tiny tags to the racket.

Scope and Limitations: Owing to our use of optical signals, FastLoc can deliver sub-centimeter accuracy only in line-of-sight and offers coarser tens of cm accuracy with non-line-of-sight (only RF). We further require the tag to be oriented in a manner that it can be illuminated by the optical projector pattern. For large objects, this limitation can be mitigated by placing multiple optical sensors or multiple tags at different orientations. We are further limited to a range of 5 meters owing to the low-cost optical projectors we use, while we can localize tags in NLOS up to 10 meters range. Note that while this implementation of FastLoc uses visible spectrum for ease of demonstration and visualization, we discuss extending FastLoc to work in the infrared (IR) spectrum in Sec. 8. We also note that the current implementation of FastLoc has compute latency which can be further optimized with dedicated hardware, we discuss the end-to-end latency in Sec. 8.

We implement FastLoc using one RF transmitter and a pair of commercial projectors that are less than $100. Our ground truth is the optical Lighthouse Tracker which is widely used by many virtual reality gaming platforms. Our results reveal that:

- FastLoc's scanning latency is 0.51 ms (see Sec. 7.1).
- FastLoc shows a median accuracy of 0.7 cm in locating multiple tags in the line-of-sight.
- Customized battery-free analog FastLoc tags consume a power of 150 uW.

Contributions: FastLoc's core contributions include:

- A novel cross-technology battery-free backscatter tag that leverages optical+RF signals for localization.
- An ultra low-latency (sub-millisecond) localization system that leverages RF wideband harmonics and a novel static projected optical pattern.
- Detailed experimental evaluation demonstrating sub-centimeter accuracy.

2 RELATED WORK

2.1 RFID/Backscatter Localization

We have seen rich literature on developing wireless techniques to localize low-power devices, such as commercial battery-free tags [21–23, 51, 54, 60, 61] and custom RF backscatter [15, 16, 25, 29, 33, 50, 53]. These systems traditionally have errors ranging from few centimeters to tens of centimeters. While past work tries to push the limit of localization accuracy by stitching the wireless channels at various frequencies over time [30, 33], these systems only work with static targets as hopping frequencies over a large spectrum takes a few seconds. Other systems build backscatter tags and passive reflectors for mm-wave that offer higher bandwidth, but nevertheless, have errors of few centimeters [18, 38, 48, 56] owing to tag form factor or are restricted to only tracking as opposed to localization. More recently, novel systems have been proposed to significantly reduce the latency of localization systems to tens of milliseconds. However these systems either require using multiple antennas on the backscatter tags [33] or using multiple RF transmitters by scanning over the different spectrum [28]. Other systems that combine RF with out-of-band acoustic sensing for localization only achieve accuracy on the order of

10 cm at a higher cost/complexity for localization and are typically limited to tracking [19, 39]. While visible light-based systems have been proposed to offer few centimeters accuracy and reduced latency in localization, these systems require strictly line-of-sight communication environment, power-hungry cameras [26, 63], or customized battery-powered and bulky photodiode-based circuitry involving sophisticated computing on the edge device [57, 64]. Perhaps closest to our system is [43] that uses LED-equipped WISP tags to aid tracking from robotic platforms, yet requires close proximity of the reader (1.5 - 2 meters) and sufficient latency to power the tag to the desired level and capture LED flashing responses by a camera. This system is strictly line-of-sight dependent despite combining RF and optical sensing methods. In contrast to all these systems, FastLoc aims to achieve sub-millisecond latency and sub-centimeter accuracy from a coin-sized passive tag by only using one single-tone RF transmitter.

2.2 Optical Tracking

OptiTrack [17] is one of the most standard high-resolution optical tracking solutions. While these motion capture technologies provide good latency, sub-centimeter tracking accuracy and use passive retro-reflective optical trackers, they require sophisticated hardware and arrays of expensive cameras. Lighthouse [11] has been widely used in AR/VR applications [20, 35, 47], it relies on mechanically steering multiple infrared line scanners to localize the trackers and headsets. While Lighthouse is relatively low-cost (~ $300) and performs millimeter-level accuracy, it does pose high latency for a wide-area scanning. Although recent research work builds customized optical infrastructure to improve the latency, it does sacrifice the localization accuracy, add complexity to the optical projector, and require battery on the optical tags [42]. An alternative optical design is to project different frequencies/colors along *all* directions at once using a commercial optical projector. While this avoided the mechanical steering of the optical source, this approach was constrained by the low-cost and low-power requirement for our tag. For instance, we could attach about two photo-diodes ($0.5 each) on the battery-free tags. However, the two photo-diodes can only collectively recognize about 8000 distinct colors due to its much lower sensitivity to colors, compared to a camera. Thus, this approach only provided the mm-scale localization resolution if the tag is known to be within a very small space (0.64 m^2). This motivated us to explore an RF-based system to coarsely locate the tag first at about few tens of centimeters of accuracy. In this paper, we seek to achieve extremely low latency and high accuracy by building battery-free tags and reducing search space for the optical scanners. Key to our approach is a hybrid design of an optical-to-RF backscatter system.

2.3 Real-Time Tracking

There is rich literature on real-time tracking systems for augmented reality. Bar-code based systems such as April Tags [52] have been a preferred high-resolution system to serve as passive fiducial markers, have relatively large form factors and offer centimeter-scale positioning [36]. Non-passive solutions based on BLE [13, 45], UWB [32], etc. have also been proposed. Various active [41, 46] and passive [37] systems have been proposed for tracking, indoor interactions, and sports applications such as ball-tracking where real-time localization is crucial. The passive systems in particular often require expensive camera platforms, akin to OptiTrack [24]. FastLoc complements this rich prior work by offering a system that is low-cost, mm-accurate, passive and achieves ultra-low latency.

3 OVERVIEW OF FASTLOC

FastLoc's objective is to achieve location and tracking at high-accuracy (few mm) and ultra low latency (on the order of near over-the-air round-trip-time). In this section, we present our architecture design and research challenges that the rest of this paper addresses.

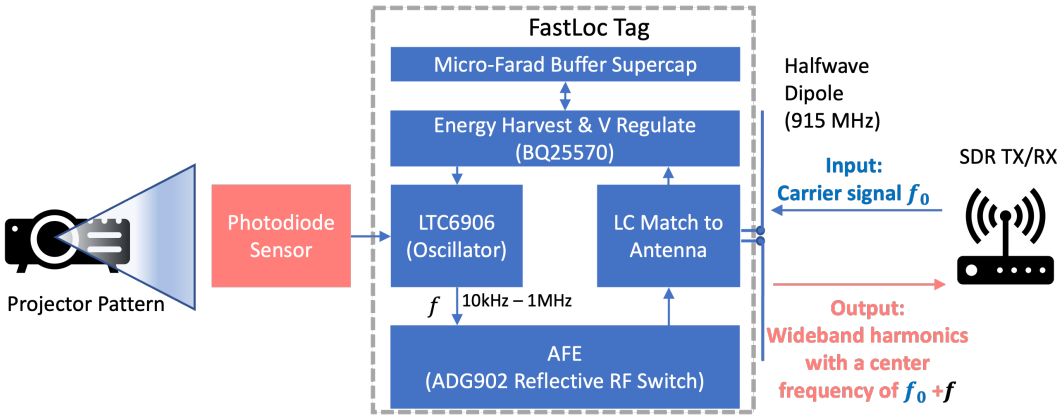

Fig. 2. Block Diagram of the Battery-free FastLoc Tag. The tag communicates observed optical color as corresponding frequency modulation backscatter with wideband harmonics. Each tag is designed to harvest energy from RF signals incident on its halfwave dipole antenna. The nanopower Buck-Boost charger (BQ25570) regulates voltage and buffers charge in a tiny ceramic μF supercapacitor. Harvested energy is sufficient to power the FastLoc tag whose power budget is lower than 150 μW at 2.3 V. For sensing, the on-board low power oscillator (VCO) is configured to modulate its output frequency in relation to the impedance of a photodiode sensor; which in turn changes based on the sensed color. The frequency modulation output is then backscattered by driving an RF reflector switch that is connected across the antenna terminals.

3.1 FastLoc's Architecture

FastLoc seeks to localize with ultra low-latency and achieve sub-centimeter accuracy using passive, battery-free tags and low-cost infrastructure. A FastLoc tag is composed of a color-sensitive photodiode and a specially designed RF-backscatter circuit that is completely analog to ensure simplicity, low-power and low-latency (see Fig. 2). FastLoc performs a one-shot localization where light from an optical projector (with a static spatial pattern) and an always-on single-tone signal from one RF transmitter simultaneously illuminate tags. Once the tag harvests enough RF energy, it instantaneously encodes the color of the light perceived on its photodiode as frequency shifts on the backscatter response from the tag. FastLoc's objective is to use both the wireless channel information from the backscatter response and the color reported by tags to identify their tagged object's location. In the implementation of FastLoc, we attach a pair of co-located tags on the tracked object. FastLoc's architecture, as shown in Fig. 1 (b), has two phases that are both processed simultaneously at the reader: (1) Use the RF back-scatter response to identify a coarse region where the tag may be located; (2) Use the color reported by a pair of co-located tags on the object to fine-tune this location within the coarse region with an error of 7 mm (roughly about one pixel in length).

Why is FastLoc low latency?: Aside from computational latency (which is platform-dependent and can be optimized with dedicated circuitry), FastLoc is solely bottle-necked by the latency of accumulating a minimum length of I/Q samples, to resolve frequency shifts of backscattered signals in a noise-resilient fashion. Both our optical projector and reader can be designed to be always-on (or can be switched on and off as necessary simultaneously). Once the reader and projector are activated, our tag is designed to be all-analog and power up to activate an instantaneous response within 30 nanoseconds. Over-the-air time-of-flight indoors is typical of the order of tens of nanoseconds. The response from the tag is a series of analog frequency-shifted tones that can be interpreted and demodulated rapidly depending on signal-to-noise ratio, as soon as the signal is received at

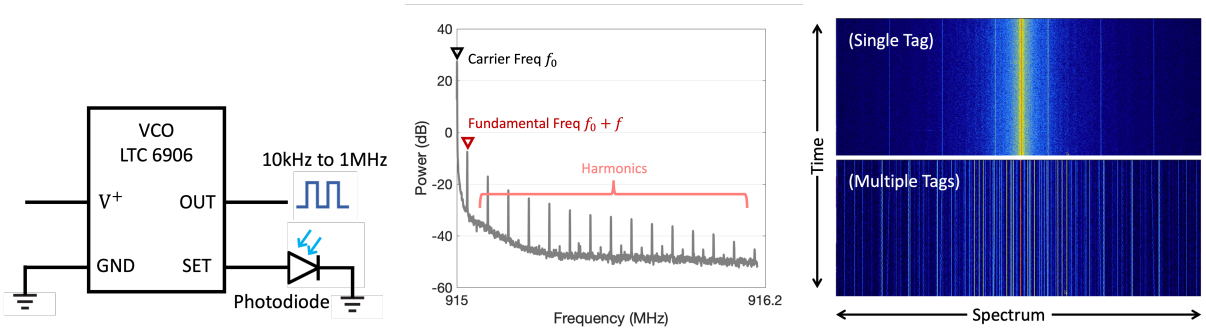

(a). VCO Connections (b). Harmonics Spectrum (c). Multiple Tags

Fig. 3. (a) The photodiode connected to the SET pin acts as a variable impedance that linearly maps sensed color to a frequency change at the VCO (LTC 6906) output. (b) Harmonics captured at the RF receiver; (c) Spectrogram of single (top panel) or multiple tags (bottom panel): the red line shows the carrier frequency.

the reader. We characterize a net latency that is sub-millisecond under diverse SNR conditions, based on our evaluations in Sec. 7.1.

3.2 Research Challenges and Outline

The rest of this paper addresses the research challenges corresponding to the RF-based coarse localization and optical fine localization of a FastLoc tag:

RF-Based Coarse Localization: We first seek to perform few tens of centimeter accurate coarse localization of the RF tag using its backscatter channel response. The key challenge here is the poor bandwidth of traditional RFID systems in a design that must by definition be ultra low-power. Sec. 4 presents our approach to remedy this by exploiting the natural harmonics that the FastLoc RF analog circuitry creates to emulate a wide bandwidth response.

Optical Fine Localization: Next, we perform fine-grained localization by leveraging the color hues detected by the tag to uniquely map to a fine-grained location within a coarse region, that is defined in the RF phase. The main challenge here is that the projector pattern must be static and known prior to the RF-localization phase. The key property of this spatial pattern is the ability to map every possible fine-grained location of the tag in the field of view to a specific color code, regardless of where the coarse grained region from the RF sensing phase is centered in the area of interest. Sec. 5 describes how we address this challenge by designing cellular-inspired spatial optical patterns that achieve this.

4 RF-BASED COARSE LOCALIZATION

FastLoc aims to minimize the search space for the future optical scans without adding latency. To do this, FastLoc estimates a coarse region where the tag may be located by leveraging its wideband harmonics. In this section, we describe how FastLoc generates wideband backscatter responses that provide tens of MHz bandwidth for coarse localization.

4.1 Leveraging Wide-band Harmonics

At the first glance, receiving a wide-band tag response can be realized by hopping across a wide range of frequencies from the RF transmitters. While location resolution can be improved by stitching a virtual wide

bandwidth, this method leads to a high latency which goes against FastLoc's objective. Instead, FastLoc only sends single-tone carrier from the RF transmitter. FastLoc's key approach is to leverage the natural harmonics that are generated at the RF tag in response to this carrier signal to generate a wide-band response. While traditionally, these harmonics are suppressed in RF circuitry to avoid leakages into unintended bands – FastLoc leverages these harmonics to its benefit. We elaborate on our approach below:

FastLoc Tag Design & Generating the Wide-band Harmonic Tag Response: To obtain the wide-band harmonic tag responses, FastLoc designs a simple battery-free tag only using analog components. Figure 2 shows the circuit block diagram of the FastLoc tag. FastLoc tags harvest wireless energy using its 915 ISM band antenna.The tiny on-board super-capacitor [2] (~50 uF) buffers sufficient energy to provide a steady 2.3V supply for the voltage-controlled oscillator (VCO) and the RF switch to operate. The VCO (LTC6906 [6]) is configured to vary its output frequency corresponding to changes in its base current consumption. Thus the frequency output of the VCO is controlled by the changing impedance of the on-board sensor (e.g., photodiode) connected across the base current node of the VCO and ground (see Fig. 3 (a)). The VCO maps the impedance of the photodiode into frequency output in range 10 kHz to 10 MHz. Then the VCO-generated square wave signals are fed to the gate terminal of an analog RF switch where the harmonics are naturally generated. The RF switch acts as a mixer that combines VCO-generated low-frequency square waves, whose frequency is controlled by the photodiode, with the carrier and backscatters them. Mathematically, an ideal square wave can be represented as an infinite sum of sinusoidal waves in the time domain:

$$s(t) = \frac{4}{\pi} \sum_{k=1,3,5,..}^{\infty} \frac{1}{k} sin(k\omega t), \text{ where } \omega = 2\pi f \tag{1}$$

f is the fundamental frequency of the square wave, in other words, the switching speed of the RF switch. Ideally, the square wave only contains components of odd-integer k harmonic frequencies and the spacing between them is $2f$. Then these baseband harmonics are mixed with the carrier signal at 915 MHz (f_0), the fundamental frequency of the harmonics shifts to $f_0 + f$. After this step, the two-sided wideband harmonics are generated around the center frequency. Fig. 3 (b) shows a representative trace of harmonics observed in the frequency domain.

4.2 Coarse Localization using Harmonics

Next, FastLoc infers the coarse location of the battery-free tag based on the one-shot wideband harmonic tag response. Indeed, FastLoc must estimate the frequency-selective fading effect experienced by the wideband harmonics along the different paths the signal traverses as it reflects off various objects in a dense indoor environment.

Resolving Multipath: FastLoc uses super-resolution Multiple Signal Classification (MUSIC) [44] to resolve the direct path from multi-bounce paths, and measuring the time-of-arrival to infer the coarse location of FastLoc tags. Mathematically, we write the steering matrix that represents wideband harmonic channels at any time τ as:

$$\mathbf{a}(\tau) = \left[e^{j2\pi(f_k - f_1)\tau} \right]_{k=1,3,5,\ldots,2N-1} \tag{2}$$

where N is the number of frequencies we applied to the MUSIC algorithm including the fundamental and its harmonics, and N can be up to 100 within 20 MHz, f_1 is the fundamental frequency, and when $k > 1$, f_k is various orders of the harmonics.

We then estimate the locations of local maxima (peaks) of $P(\tau)$ to obtain the measured time of arrival of the wideband harmonics, where $P(\tau) = 1/[\mathbf{a}(\tau)^{\dagger}\mathbf{E}_n\mathbf{E}_n^{\dagger}\mathbf{a}(\tau)]$, $\mathbf{E}_n$ are the noise eigenvectors of the correlation matrix of the observed wireless channels of the tags and $(.)^{\dagger}$ is the conjugate-transpose operator.

Finding Coarse Tag Region: The coarse location of the tag is measured at the time-of-flight corresponding to the nearest dominant reflection (assuming line-of-sight). We receive signal measurements from three spatially separated MIMO reader antennas to trilaterate the tag's position. Empirically, we observe a 95^{th} percentile error in position of 38 cm of our RF-based coarse localization component across varied experimental conditions (SNR, orientation, etc.) as we describe in Sec. 7. We therefore conservatively define the coarse tag region as a circle centered at the location found by this algorithm and a radius of 38 cm.

> **Take-Away # 1:** FastLoc exploits the natural harmonics generated by low-cost analog tag circuitry to generate a wide-band localization-friendly RF response from inexpensive tags for coarse localization.

4.3 Dealing with Multiple Tags

While so far, our discussion considers a single FastLoc tag in the environment, the presence of multiple FastLoc tags would considerably change our received signal. Specifically, these wideband harmonics from multiple tags will scatter over a significant spectrum, and possibly overlap with each other. As a result, FastLoc must disentangle the harmonics for each tag before inferring the coarse location of each tag.

While one may think of allocating the fundamental frequency of each tag in separate frequency bands to mitigate interference and overlap, higher orders of one tag's harmonics will inevitably fall into other tag's allocated frequency band (see Fig. 3 (c)). Hence, this method alone cannot guarantee to separate all the harmonics. As a result, FastLoc first allocates each tag within separate frequency bands, and then formulates an optimization algorithm to progressively discover the set of frequency responses (fundamental plus harmonics) for each tag starting from low frequencies (closer to the carrier frequency) to the higher ones (further away from the carrier). Specifically, FastLoc leverages the fact that if the fundamental frequencies are different for each tag, the harmonics spacing s will be unique among the tags. Thus, FastLoc can generate a set of harmonic patterns S_i for each tag i. FastLoc then searches for the best-fit generated harmonic pattern with the observed wireless channels for each tag. Mathematically, we obtain the best-fit pattern with a spacing of s^* between adjacent harmonics for tag i by solving the following optimization:

$$s^* = \arg\min_{s \in S_i} \sum ||H_{\text{est}}(s) - H_{obs}(s)||^2 \tag{3}$$

where H_{est} is the generated harmonic pattern by using the Eq. 1 in frequency domain, and H_{obs} is the observed wireless channels in frequency domain. The above is a standard least-squares optimization and can be solved in polynomial-time. We, therefore, apply this method to progressively extract the frequency responses from the observed spectrum for each FastLoc tag. Theoretically, FastLoc can at once support up to 180 tags within the entire ISM band at 915 MHz – allocating 150KHz bandwidth for each tag's fundamental frequency. This implied that within a given area of interest we can deploy up to 180 tags. In our experiments, we deploy eight FastLoc tags in the environment to simultaneously locate them using FastLoc's algorithm above.

5 OPTICAL FINE LOCALIZATION

In Sec.4, FastLoc estimates a decimeter region of the tag's location based on their one-shot wideband backscatter responses. Although the wideband harmonics give a coarse location of the tags at an ultra-low latency, the location accuracy purely relies on RF responses is not sufficient for applications like virtual reality. Traditionally, commercial VR systems [11, 12] locate photodiode-mounted trackers by steering multiple horizontal and vertical

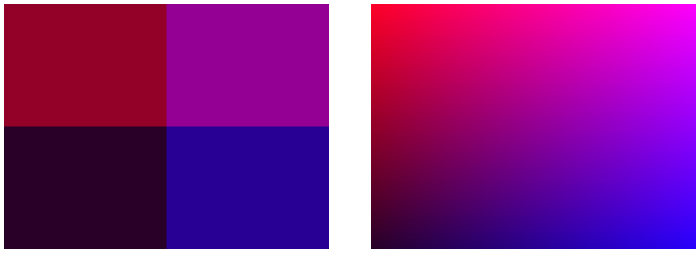

(a). 2 × 2 Grid (b). 100 × 80 Grid

Fig. 4. (a) Evenly splitting the area by four frequencies/colors; (b) Evenly splitting the area by 8000 unique frequencies/colors;

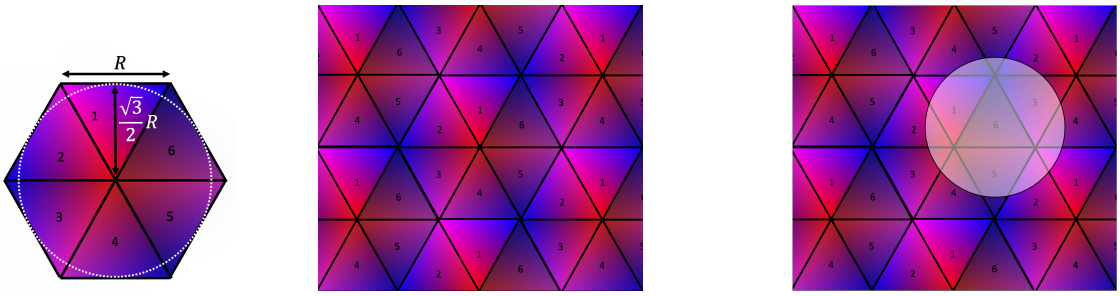

(a). Single Hexagon (b). Projected Color Pattern (c). Inscribed Circle.

Fig. 5. (a) A single hexagon distinct colors. The hexagon has six sub-regions each with different levels of intensities. The inscribed circle (dotted white) encapsulates the maximum possible area of the coarse region. (b) The hexagon is tiled to form the projector pattern. (c) The inscribed circle can be moved along freely across the grid without having more than one pixel of the same color within its bounds. Note that the actual projected image does not have any black or white annotations shown above.

line lasers mechanically over the space of interest, but subject to mechanical steering latency (~ 32ms for 3D scans). This section describes how FastLoc tracks the location of tags at near over-the-air round-trip-time latency and sub-centimeter accuracy by applying a single, static color pattern using commodity optical projectors. Specifically, we target a latency that is sub-millisecond – around the time duration required to collect sufficient I/Q samples to receive and decode the backscattered tone at even moderate to low SNRs and remain robust for speeds up to 50 km/h of objects indoors, such as spinning motor parts (see Sec. 7).

5.1 Optical Spatial Multiplexing

The key idea of performing a fine-grained localization of FastLoc tags is to illuminate unique frequencies of optical signals spread over the entire space of interest. In other words, we apply spatial multiplexing using highly directional optical signals. For example, let's consider a $2D$-space area divided into a 2×2 grid, and project four different frequencies (colors) in each section (see Fig.4 (a)). Colors can be represented using a 3-tuple RGB (red, green, blue) values in the range 0 to 255. In Fig.4 (a), the colors are (20,0,20), (120,0,20), (120,0,120), (20,0,120) for bottom-left, top-left, top-right, and bottom-right respectively. Note that we use optical signals in the visible spectrum range for these experiments here, but this can easily be adapted to a system which uses a range of frequencies in the Infrared band along with corresponding IR receiver photodiodes on the tags.

Now, if the tag can sense the color of the light that illuminates it and backscatter this color information back to the receiver, FastLoc can infer in which of these four sections the tag is located. Naturally, rather than restricting to only four quadrants, we can instead project a larger number of colors with an extremely high resolution. Fig. 4 (b) shows a 100×80 grid with each section displaying an entirely different color. As a result, FastLoc can locate the tag with a much better spatial resolution, since each pixel spans an extremely small area. However, in practice, to ensure low tag cost and power consumption, a FastLoc tag can only sense a limited number of distinct colors. Thus, we cannot simply divide the projected area into extremely small pieces. For instance, the number of unique colors for each tiny pixel, e.g. a 1080p LCD projector has a 1920×1080 pixel resolution (2,073,600 pixels in total). In our implementation, we use two photodiodes that respond to two distinct colors – red and blue to ensure tag simplicity. While in principle, we could use three or more colors, we restricted our system to two to limit energy needs and ensure tag simplicity. Each photodiode was low-cost and low-power and can disambiguate about 8000 distinct colors at high precision under ambient noise – the various shades that mix blue and red as shown in Fig. 4 (b). As described in Sec. 2.2, this translates to a small overall physical area when projected ($\sim 0.64\ m^2$) to achieve a sub-centimeter scale for each pixel.

5.2 Designing the Projector Pattern

At this point, we need to design the pattern from the projector that ensures that the coarse region of the tag from the RF measurements can be fine-tuned to within one or two pixels. The challenge however is that we do not know up front what the coarse tag location is – otherwise our system would require two round-trip times and additional processing latency. A naive approach would be to simply tile the pattern in Fig. 4 (b). However this approach may be sub-optimal given abrupt color transitions at the boundaries between tiles that make the system less robust to noisy measurement.

We therefore seek to find a near-optimal spatial projected pattern that makes best use of our available 8000 colors to ensure maximum possible localization accuracy. Such a color pattern needs to have the following basic requirements: (1) Any two pixels with the exact same color should be as far away as possible – specifically, by at least D, the diameter of the coarse tag region circle (see Sec. 4.2); (2) Colors of adjacent pixels should be highly correlated over the entire projected image. The first property makes sure that regardless of where the coarse region (error circle) is located, it encompasses only unique colors and we are guaranteed no ambiguity in location. The second property ensures that even a modest error in color measurement leads to distance error of just a few pixels.

Goal 1: Maximize minimum distance between same-colored pixels. FastLoc designs a hexagonal tile pattern inspired by cellular network design that reuse frequencies (colors in our context) in geographical areas (in different hexagons)[31]. Within a single hexagon, no colors will be reused. Similarly, FastLoc designs each hexagon to have all distinct colors that can be sensed by the FastLoc tags (see Fig. 5 (a)). The surface area of each hexagon is determined by the estimated RF coarse region. To see why, consider a coarse region whose diameter is the same as that of the inscribed circle within any of the hexagons as shown by the dotted circle in Fig. 5 (a). Note that since this circle is entirely within the hexagon, it has no duplicate colors. Further, one can show that no matter where the inscribed circle is moved along the plane, it continues to only have distinct colors within it (see Fig. 5 (c)). This directly follows from the fact that the closest pair of pixels of the same color in the entire grid are (approximately) at opposite edges of the hexagon – where the inscribed circle intersects the hexagon. In other words, as long as the diameter of our coarse region circle D is equal to (or below) the diameter of the inscribed circle, we can ensure no ambiguity in the position of the tag.

Our specific hexagonal pattern is also near-optimal in terms of supporting as large a value of D as possible as dictated by the number of distinct colors the projector can generate. Let us denote the efficiency α of our scheme

as the fraction of the diameter of the inscribed circle with that of the diameter of an optimal circle that contains all the possible distinct colors our tag can differentiate.

THEOREM 5.1. *The efficiency α of FastLoc's hexagonal pattern is: $\sqrt{\pi/(2\sqrt{3})}$ or approximately 95%.*

Proof Sketch: Recall that each of our hexagons has the same area as the optimal circle, since it encompasses all possible distinct colors as well. It is then easy to see that the ratio of the areas of the inscribed circle and hexagon is simply α^2. Using simple geometry, we can write this as:

$$\alpha^2 = \frac{S_{\text{circle}}}{S_{\text{hex}}} = \frac{\pi(\frac{\sqrt{3}}{2}R)^2}{6 * \frac{\sqrt{3}}{4}R^2} = \pi/(2\sqrt{3}) \tag{4}$$

where R is side length of the hexagon.

Goal 2: Adjacent colors should be highly correlated. To address this requirement, FastLoc further divides the single hexagon into six blocks as shown in Fig. 5 (a). All blocks in one cell have distinct colors. Also, the averaged color intensity (brightness) of each block is gradually decreasing shown in Fig. 5 (a) from block 1 to block 6. By doing this, FastLoc can tolerate modest tag signal measurement errors which in turn causes minimal errors at the boundaries of hexagons.

> **TAKE-AWAY # 2:** FastLoc develops a near-optimal color pattern that can be used to illuminate the tag to fine-tune its location based on sensed light color without prior knowledge of the coarse region from RF.

5.3 Sensing Colors Using FastLoc Tags

Next, we describe how we use FastLoc tags for color sensing only using ordinary photodiodes. We design analog battery-free tags that are highly responsive to optical signals. Specifically, we connect photodiodes on tags as the on-board sensor. The impedance of the photodiode changes with the incident optical signal so that it can modulate the optical information on the frequency of its backscattered signal — shifting the fundamental frequency and the wideband harmonics of the tag signal through a low-power VCO (see Sec. 4.1 for details). While the spectrum of a typical photodiode is usually wide from blue (wavelength: 400 nm) to red colors (720 nm), it only has a one-on-one mapping between the light illuminance and its resistance. Thus, a typical photodiode cannot distinguish colors. FastLoc, therefore, creates color-filtered photodiodes by simply attaching transparent red/blue plastic film sheet on top of the photodiodes so that each color-filtered photodiode is only responsive to individual colors – red or blue in our case. In Fig. 6 (a), we show the frequency shifts of two co-located tags with blue-filtered and red-filtered photodiodes respectively when the FastLoc projector projects only shades of red. Therefore, FastLoc can use different co-located color-filtered photodiodes to reconstruct precise color that illuminates the FastLoc-tagged object.

5.4 Mapping Colors to Location

Mapping of Frequency Shifts to Colors: Since we attach extra color-filters on the photodiodes, we cannot rely on the one-on-one mapping of the photocurrent and the optical irradiation provided by the manufacturer. Thus, FastLoc collects all the frequency responses as projecting designed colors to the color-filtered photodiodes. Once the data is collected, we create a model that maps the frequency shifts to colors. Statistical curve fitting has been used to avoid over-fitting and interpolate the model. Note that our model subtracts out the frequency shifts of the background light so that FastLoc removes the influence of the ambient light. FastLoc only needs to collect the mapping once after attaching the extra layer of colored filters on the photodiodes. The one-on-one relation

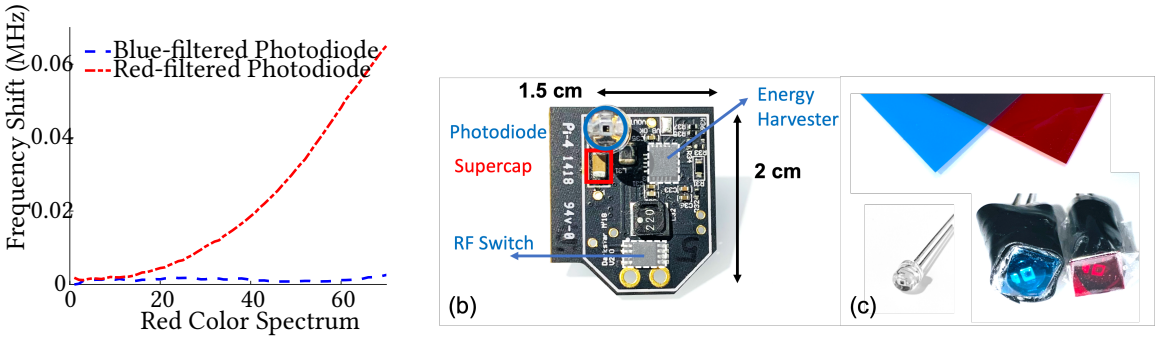

(a). Frequency Responses of PDs. (b). Tags; (c). Photodidoes;

Fig. 6. (a) Frequency responses of color-filtered FastLoc tags when the projector projects shades of red. (b) Battery-free FastLoc tag (without antenna). Oscillator and LC match on the backside of PCB. (c) Blue-filtered and red-filtered photodiodes have blue and red gel filters attached on top of the wideband visible light photodiodes [10]. In our implementation, we attach one color-filtered photodiode sensor on each FastLoc tag. An object can be localized by attaching a pair of co-located red/blue photodiodes-equipped FastLoc tags on the object.

between the frequency responses and the color is independent of the ambient light environment. The whole collection process requires less than 1 minute for a fine-grained color collection.

Object Localization: To localize an object, we attach a pair of co-located FastLoc tags on the object. Each tag is equipped with one red or blue-filtered photodiode. FastLoc locates the object by measuring the frequency shifts of both red and blue-filtered photodiodes. After subtracting out the frequency shifts induced by the ambient light, we compare the measurement with our color-to-frequency map to determine the color projected on the co-located tags. Using one projector, we obtain a 3D line that points at the tagged-object or the object's 2D location if it is on a known plane. Should a 3D position be desired, we can use two projectors, to obtain two 3D lines. We then use a geometric approach to find the two points on these lines that are closest to each other and use the middle of the intersection as the final result.

6 IMPLEMENTATION

FastLoc Tag: At the heart of FastLoc is a novel analog and battery-free wideband harmonic backscatter tag described in Sec. 4.1. We design and fabricate the FastLoc tag based on the architecture proposed in [40]. FastLoc uses purely analog components in the hardware to ensure simplicity and low-power consumption. It supports a communication distance up to 10 meters with an LC-matched half-wave dipole antenna. Across all experiments, we use the custom half-wave dipole antenna resonating at 915 MHz with a 3 dBi gain. The dipole antenna has a length of 13 cm and can be fabricated flexibly to integrate into objects. While the FastLoc prototype uses a PCB dipole antenna on the tags due to its ease of custom fabrication, we note that our battery-free FastLoc tag could integrate with commercially available 915 ISM band compact antennas (e.g., Amphenol's PCB antennas [1] have a dimension of 60 mm × 15 mm × 0.8 mm, and Linx's ceramic patch antennas [5] have a dimension of 25 mm × 25 mm × 4 mm). FastLoc tags have a power consumption less than 150 μW, and respond with a latency less than 30 ns. Fig. 6 (b) and Fig. 1 (a) depict a prototype of our hybrid Optical-RF tags. In each experiment, we use a pair of co-located tags for localization, and each tag is applied with red or blue colored gel filters (Fig. 6 (c)) [4].

FastLoc Station: We have a low-cost 915 MHz RF transmitter module that constantly sends a single-tone carrier signal that also serves as the energy source to the tags in the environment. We use two LCD projectors (Pansonite

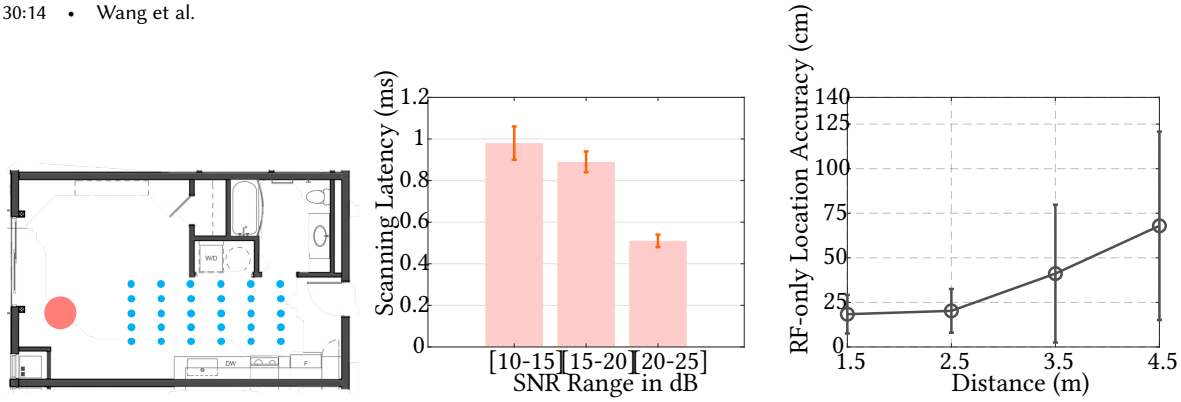

(a). Experiment Environment (b). Scanning Latency (c). RF-only Localization

Fig. 7. (a) Layout of the environment (10 × 6 m) for experiments, the red dot represents the location of the FastLoc station, blue dots represent the example locations of the FastLoc tags. (b) FastLoc has a 0.51 ms scanning latency in locating the FastLoc tags under a 25dB SNR. (c) Baseline 2: FastLoc's RF-only localization shows a 31 cm on average.

Mini Projector [8] which has 1280 × 720 display resolution) to project our designed color patterns into the coarse region inferred by the wideband RF harmonics. On the receiver side, we have two X310 USRPs with three antennas to estimate a coarse location, and they also process the optical responses (to the optical projector pattern) modulated within the RF signals.

FastLoc Software: All software processing occurs solely within the FastLoc station. FastLoc's RF front end includes signal transmission and reception and is implemented using C++. Optical projection and other FastLoc localization algorithms are fully implemented in Python.

Ground Truth and Baseline: We use Lighthouse base stations (version 1) and a Lighthouse tracker as the ground truth. The Lighthouse tracking system is a laser-based tracking system developed by Valve for SteamVR and HTC Vive. We compare FastLoc against two baseline systems: (1) **Baseline 1:** A location tracking system that does not perform RF coarse localization in the first place, but directly projects the a naive optical patterns throughout the whole space (e.g. Fig.4 (b)). (2) **Baseline 2:** A RF-only location tracking system that localizes the tags using wideband harmonics. We note that unless specified otherwise, error bars in graphs denote standard deviation.

7 RESULTS

7.1 Scanning Latency

There are three main components that contribute to the scanning latency of FastLoc: (1) time-of-flight between the FastLoc station and the tags; (2) modulation latency at the tag; (3) the delay in accumulating a few I/Q samples to then apply FastLoc algorithms. Of these, the last one primarily bottlenecks scanning latency:

Over-the-air Time-of-flight: This quantity captures the time that RF backscattered signal travels from the tag to the FastLoc station. Since our tracking volume spans a space of 4.5 × 4.5 × 4.5 meters, the latency of the time-of-flight would be less than 26 nanoseconds.

Modulation latency on the FastLoc tag: The latency of the FastLoc tag operation is mainly introduced by the response time of the on-board oscillator that produces a periodic baseband square wave at a particular frequency that is dependent on the color sensed by the photodiodes. The on-board oscillator we are using has a worst case response time of 20 ns [7] at our operation voltage (2.7V). The second component of on-tag latency is the propagation delay of the RF switch which adhttps://www.overleaf.com/project/5f78b87ed0957800013016c2ds

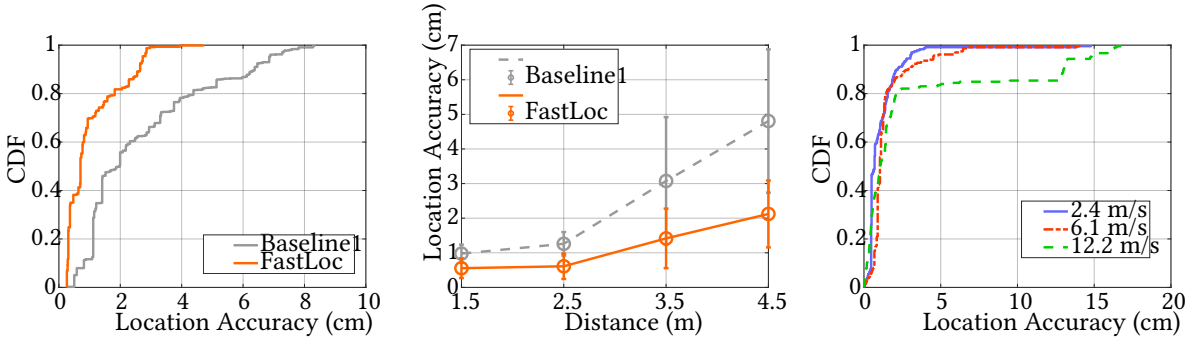

(a). CDF of Location Accuracy (b). Accuracy vs Distance (c). RF-only Coarse Estimation

Fig. 8. (a) FastLoc achieves a median accuracy of 0.703 cm in locating the battery-free FastLoc tags, a 65% improvement comparing to a 19.8 mm median accuracy of the Baseline 1 which does not perform the RF coarse localization. (b) With a distance of 4.5 meters from the FastLoc station, FastLoc achieves an average accuracy of 2.1 cm to localize the tags. (c) FastLoc achieves a 1.1, 1.4, 3 cm mean accuracy when tags move in a speed of 2.4, 6.1, 12.2 m/s.

a worst-case switching delay of 9.5 ns at the operating voltage [9]. Hence the overall on-tag latency is a only around 30 ns.

Accumulating a few I/Q samples: Note that FastLoc needs to accumulate a few I/Q samples in order to obtain the precise frequency shift of backscattered signals in a noise-resilient fashion. In other words, we need to accumulate a minimum length of I/Q traces to properly resolve the frequency shifts (few kHz apart) and map them into the set of distinct hues of red and blue colors. Specifically, the minimum length depends on the Signal-to-Noise Ratio (SNR) of the received tag signals. Note that a FastLoc tag reflects multiple copies of the signals simultaneously (wideband harmonics) which can even improve the SNR. Fig. 7 (b) plots the aggregated scanning latency of FastLoc systems. We show that FastLoc are able to provide a 0.51 ms latency (~ 2kHz) under a 25 dB SNR on average. Note that this is still a significant improvement over the scanning latency of 16 ms for the Lighthouse tracking system that mechanically steers laser light.

7.2 RF-only Coarse Localization

Method: This section describes the evaluation of the RF-only component of FastLoc localization performance (Baseline 2). Note that FastLoc uses the RF sensing phase 4.2 to estimate the detected tags' coarse region. FastLoc achieves the one-shot decimeter-level coarse localization by leveraging analog tag's wideband harmonics. We deploy the tags in an indoor, multipath-rich environment without any projected pattern from the optical projectors and evaluate the location accuracy up to 4.5 meters between the FastLoc station and tags.

Results: Fig. 7 (c) shows the 3-D location accuracy of RF-only coarse estimation. We observe a 31 cm averaged accuracy, and errors of 18.4, 20.2, 41.1, and 67.94 *cm* on average at 1.5 to 4.5 meters respectively. In the experiments, we apply 20 MHz wideband harmonics to our localization algorithm. Note that, the harmonics can expand as much as 50 MHz bandwidth dependent on the channel conditions, which is available to us to further improve the RF location performance. In FastLoc, we conservatively use the 95^{th} percentile error of the RF location accuracy as the radius of the coarse region, which then be used to define a single hexagon to generate our colored pattern that guarantees no ambiguity in optical fine localization within the coarse region.

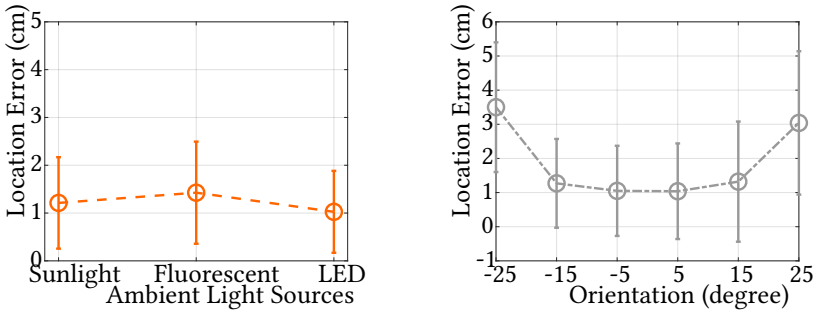

(a). Impact of Ambient Light (b). Impact of Orientation

Fig. 9. (a) FastLoc has a mean accuracy of 1.212, 1.426, 1.0185 cm in locating the FastLoc tags under different sources of ambient light. (b) FastLoc remains robust when the angle of tag's orientation is within the half sensitivity of the on-board photodiode.

7.3 Accuracy of Localization

Method: We deploy the FastLoc station and four pairs of FastLoc tags in a 6×10 meter studio which is a typical environment for AR/VR gaming applications. Note that each pair of tags are co-located, and has one red-filtered and blue-filtered photodiode respectively so that we can use them jointly to infer their location. We try various locations, orientations, and altitudes (0.5-2 m from the ground) of multiple tags as shown in Fig. 7 (a), with different lighting conditions in the environment (e.g. 5, 15, 35 lux). For all these 3-D localization experiments, we use two projectors and project our designed color pattern in a time-multiplexed manner.

Results: Fig. 8 (a) shows the CDF of location accuracy for both FastLoc, which projects our designed color pattern, and the Baseline-1 which naively projects all distinct colors through the whole space. FastLoc has a median error of 0.7028 cm in locating multiple FastLoc tags simultaneously. We note that it is able to locate the FastLoc tag much more accurately than the baseline-1 approach, which has a significantly larger size of the color pixels as the distance increases. Overall, FastLoc outperforms the baseline-1 and the baseline-2 (RF-only) in location accuracy by $2.8\times$ and $44\times$ respectively.

Accuracy under Various Lighting Conditions: We conduct experiments to evaluate the impact of ambient light. Specifically, we deploy our system under different types of ambient light environment: sunlight, fluorescent lamps, and LED. These light sources have different ranges of wavelengths. The color temperature of the LED light bulbs and the fluorescent lamps is 3000k and 6000k respectively. For different lighting conditions, we try various locations and orientations of the tags. Fig. 9 (a) shows the FastLoc's location accuracy across various lighting conditions. As expected, we observe that FastLoc's performance remains robust under the sunlight, fluorescent lamps, and LED lighting conditions (a mean error of 1.212, 1.426, and 1.0185 cm respectively). We note that while the applied light sources have different visible light wavelengths, their spectrum is significantly wider than the color spectrum of our projected optical pattern. Thus, FastLoc's algorithm can treat these light sources as wide and flat background noise and subtract out the frequency shifts induced by the ambient light when reconstructing the colors using the blue and red photodiodes.

Impact of Orientation: We evaluate the impact of the tag orientation on the localization accuracy of FastLoc. We use the projector lens plane as the reference plane and place a pair of co-located tags at various locations (fixed altitude and max distance at 3.5 m) with different azimuth angles with respect to the reference plane. In our experiments, we define 0° in azimuth as the co-located blue and red photodiodes face the projector lens. We rotate the pair of co-located tags with its azimuth angle varying from -25° to 25° in steps of 10°. Fig. 9 (b)

shows the results of localization accuracy with different tag orientations. We observe that as the tags orient to a large angle (e.g. 25°) w.r.t the projector, the system performance drops. We note that this is because our low-cost photodiodes [10] have a limited field of view: the angle of half sensitivity of the photodiodes have an approximate 40°. However, our localization error at even the poorest object orientations has a mean accuracy of 3.25 cm. Possible approaches to resolve this challenge is to use multiple pairs of co-located color-filtered photodiodes on the tracked object.

7.4 Impact of Distance

Method: We evaluate the impact of various distances of the FastLoc tags on the 3-D localization performance of FastLoc. Specifically, we deploy eight FastLoc tags at several spots at distances of 1.5, 2.5, 3.5, and 4.5 meters from the FastLoc station. Note that the tracking volume of FastLoc is approximately $4.5 \times 4.5 \times 4.5$ meters restricted by the brightness of the used projectors. Across experiments, we note the FastLoc tags are in the line-of-sight for the FastLoc station. Again, we compare the performance of FastLoc with baseline-1.

Results: Fig. 8 (b) shows the location accuracy vs the increase in distance and compares it against the baseline-1 technique that projects the naive color pattern (Fig. 4 (b)). We observe that for the baseline, as expected, the location error increases dramatically as the distance increases, and we see that the accuracy drops up to 8.3 cm at the distance of 4.5 meters. FastLoc, with a 0.56, 0.61, 1.416, and 2.122 cm location accuracy on average at 1.5 to 4.5 meters distance respectively, outperforms the baseline significantly. Further, we observe that the errors of FastLoc are slightly increasing as the distance increases. We note the reason might be two-fold: (1) the brightness of the projection image dims as the distance increases. While the projector we used has 2200 lumens and limits the effective optical communication range of FastLoc, this can be easily fixed with more advanced LCD, laser or infrared projectors. (2) The size of the projected color pattern/image scales with the throw distance from the projector lens. This relationship between the throw distance and the width of the image is also called throw-to-width ratio. In other words, the size of each pixel that is projected into the physical area scales with the distance from the projector. We can approximately observe this relation from the increased mean errors of FastLoc as the distance increases. Using a projector with a long throw ratio at a longer range could mitigate this effect.

7.5 Impact of Mobility

Method: We use a rotation platform as our testbed in an indoor, multipath-rich environment, analogous to the environment of VR/AR applications. We deploy a pair of FastLoc tags on one side of the motor part which placed 2.5 m distance from the FastLoc station. The tag is rotated in a circular motion with a constant velocity. Note that, in this section, we compute the 2-D locations of the tags. We move the tag at speeds of up to 2343 rpm or 12.3 m/s (about 45 km/h). We avoided speeds higher than 45 km/h owing to the limits of our motor and to limit safety concerns for an experiment performed indoors.

Results: Fig. 8 (c) plots the CDF of FastLoc's localization performance. Overall, FastLoc achieves a 1.11, 1.42, 2.98 *cm* mean accuracy in a constant linear velocity of 2.4, 6.1, 12.2 meters per second (which amounts to 469, 1171, 2343 rpm for the motor we used) respectively. FastLoc's robustness to mobility stems from the usage of wideband harmonics and a single tile color pattern projection which provide a ultra-low scanning latency for FastLoc. As expected, the accuracy dips in presence of mobility compared to the static use case. Indeed, we observe occasional outliers in the inference of the location when the speed reaches higher. We surmise that this is because, as the tags move fast, there are spots that the tags cannot harvest sufficient energy to operate due to the various orientations with respect to the transmitter and a fast fading effect. Note that the tags do not completely fail to operate at these spots, but instead transmit unstable frequencies back to the receiver. For example, the on-board oscillator

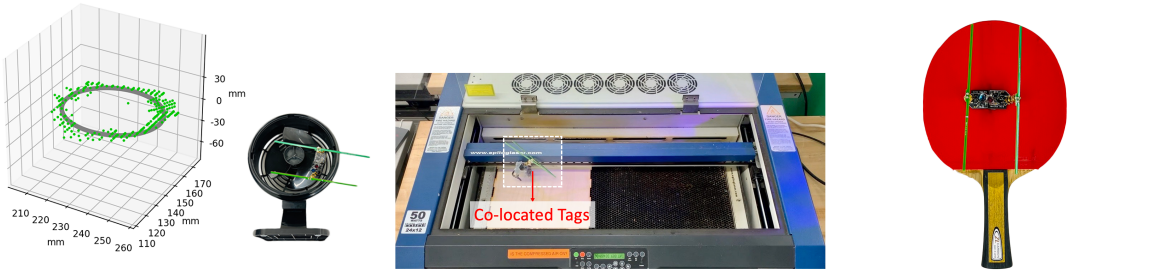

(a). Fan Spinning (b). Tracking Laser Cutter (c). Tagged Ping-pong Racket

Fig. 10. FastLoc opens up several applications described in Sec. 7.6 by tracking the trajectory of fast-moving objects, e.g., fans, the nozzle of the laser cutter, and even the tagged racket at ultra-low latency and high precision. The simple tag architecture can be miniaturized into chip form (similar to RFID tags) with printed antennas that can be integrated into the objects (eg. surface of the racket or fan rims).

may struggle to receive sufficient voltage so that it cannot output stable frequency modulation for the sensed color information. While this is common for all battery-free systems like RFID or backscatter devices, we could provide a more battery-free friendly radio environment by using blind beamforming techniques [55] – a task we leave for future work. In addition to perform well in the the current setting we note that FastLoc is limited in the refresh rate of measurements from tags in high mobility settings. Specifically, the signal to noise ratio that dictates the rate at which we could collect useful measurements, at slightly under one millisecond, as discussed in Sec. 7.1. Further, changes in orientation of the tag, spin of the tag in 3-D, etc., could impact measurements. We leave a detailed evaluation of these factors for future work.

7.6 Applications

Predictive Maintenance: FastLoc can help to prevent machine failure by detecting the first signs of trouble. We show FastLoc can be used to track the trajectory of a fast spinning fan (see Fig. 10) with a median accuracy of 8.9 mm and a 0.76 ms latency. In the demonstration, we use two tags for the showcase, we note that FastLoc's RF plus optical algorithm provides the advantage of having a high-density tag deployment in the environment to generate multiple trajectory point-clouds for predictive maintenance.

Motion Tracking for Industrial Manufacturing: Manufacturing plants are full of moving parts. For example, an automated robotic vehicle assembly pipeline which operates at high speed to meet vehicle demands. In such cases, the combination of fast-moving machinery, equipment, robots, and vehicles mean that manufacturing plants can be dangerous places. FastLoc provides a way for manufacturing employees to have a safer environment by tracking the motion of fast-moving machinery at ultra-low latency. The coarse RF estimate from FastLoc can also help locate potential problem areas that need finer inspection with the optical method. We evaluate FastLoc by tracking the nozzle of laser cutter when it runs in a raster engraving mode with a 4.3 mm median accuracy and 0.62 ms latency.

Fine-grained Gesture Sensing for Sports Interaction: Previous work has shown that an average person can perceive latency levels as low as 6 ms [59] when interact with game and touch screen devices. Even very low levels of latency could be discriminated by a human, i.e., 1 versus 2 milliseconds [34]. To enhance the experience of user interaction and decrease the overall latency for the interaction tools, like wireless stylus, game controllers, FastLoc is able to provide a 0.51 ms scanning latency. We show that FastLoc enables ping-pong racket tracking when the user plays ping-pong.

8 DISCUSSION

Computational Latency on an iMac: Currently, the FastLoc prototype runs on a 2017 iMac. In addition to the scanning latency, FastLoc has a computational latency mainly contributed by three factors: 1) disentangling the harmonics from multiple tags (39 ms); 2) the MUSIC algorithm that determines a coarse region of one object (0.51 s); 3) the optical algorithm that maps the frequency shifts of photodiodes to colors (3 ms). In total, FastLoc has an end-to-end refresh rate of around 1.81 Hz. Note that, we can decrease the end-to-end latency relying on the fact that FastLoc does not have to perform the coarse localization for all scanned snapshots (e.g., FastLoc has a scanning rate of 2 kHz) since the object may not move outside the coarse region between adjacent snapshots. Moreover, we note that our algorithms are implemented for demonstration using unoptimized python code which could be sped up with lower-level programming language. The end-to-end latency can be optimized further with dedicated hardware, such as FPGA, etc.

Projecting Optical Pattern Using Infrared: Even though the current implementation uses photodiodes and projectors in the spectrum of visible light that can be seen by human eyes and is sensitive to ambient light, the proposed FastLoc architecture is easily extended to infrared spectrum (850-1650 nm) which is widely used in commercial VR products. Further, both infrared photodiodes and different types of multi-spectral infrared projectors are commonly used (e.g. TV remote, FaceID, Microsoft Kinect). While commercial infrared projectors are able to generate both images and videos in the short wave infrared with spatial frequency modulation [3, 14], the algorithm of FastLoc only requires a static projection. We leave an extension of FastLoc to infrared spectrum for future work. Note that while having the optical illumination source being invisible to the human eye is an implementation advantage, it's a downside for experimentation and ease of research use. The system doesn't suffer tremendously from having to use visible light and off-the-shelf components. So part of the motivation for leaving this as future work is that the system is much easier and approachable for peer researchers to reimplement and reuse, as well as being easier to work with for experimentation. Additionally, the current static single projected pattern of FastLoc can be extended to different R/G/B hues patterns so that when they are flashed fast – alternating red, green, and blue hues of colors, the projected patterns look like ambient light for human eyes.

Impact of Ambient Light in the Environment: FastLoc periodically measures the background lighting conditions and subtracts out the frequency shifts induced by the ambient light. Then, FastLoc compares the measurement with our color-to-frequency map to determine the color projected on the co-located tags. FastLoc actively projects a known optical pattern in the environment, and the FastLoc algorithm only measures the frequency differences of each photodiode's responses. Thus, ambient light in the environment for FastLoc is treated in a manner similar to background noise in the RF space. Provided the ambient light is not sufficiently powerful to jam the optical channel of the photodiodes that leads them to be saturated (akin to RF signal clipping in the RF domain), FastLoc system remains robust to dynamic ambient light. Moreover, if the FastLoc system is extended to the infrared range the problem of ambient noise is mitigated further.

Extending to 3-D Fine-grained Localization: To localize a FastLoc-tagged object, FastLoc uses a pair of co-located red/blue-filtered photodiodes attached on the object. Each tag currently hosts one photodiode. However, future miniaturized tags can be designed to accommodate multiple photodiodes in series/parallel to leverage their respective impedance combinations and cover larger angles. For our 3-D localization experiments, we time-multiplexed two LCD projectors by switching their projector pattern rapidly, which incurs a modest few millisecond delay (can be sub-ms with more advanced projectors [58]). A better approach eliminating the switching delay between projectors is making two projectors send their illumination patterns simultaneously to two pairs of photodiodes on the object as desired either by projecting orthogonal sets of colors from two

projectors or using polarization filters on both projectors and photodiodes for multiplexing [49, 57]. We believe future implementations of FastLoc can benefit from the rich literature on visible light communication.

9 CONCLUSION

This paper presents FastLoc, a novel ultra low-latency localization system that designs a custom analog backscatter tag and an algorithm that leverages its wide-band harmonic response to localize the tag at sub-centimeter accuracy. FastLoc has applications in Augmented/Virtual Reality and industrial IoT where localization latency is pivotal. FastLoc achieves its low latency through a hybrid optical and RF-Backscatter design. FastLoc uses commodity optical projectors and an RF transmitter to illuminate the tag with a single-tone wireless signal and an intelligent optical spatial pattern simultaneously. The RF channel response from the tag is used to locate the tag within a coarse decimeter sized space and the tag's sensed optical signal is used to fine-tune its location to within sub-centimeter accuracy. FastLoc was fully implemented and evaluated, demonstrating a 0.7 cm median localization error at sub-millisecond latency. We believe there is important future work that can make FastLoc more robust to changes in orientation and blockages, as well as the potential to make the optical patterns invisible using infrared spatial patterns.

ACKNOWLEDGMENTS

We thank colleagues at Microsoft Research and anonymous reviewers for their constructive feedback. We would like to thank Microsoft Research Fellowship and NSF (grants 2030154, 2007786, and 1942902) for their support.

REFERENCES

[1] 2021. Amphenol PCB Antenna. https://www.mouser.com/datasheet/2/18/1/Amphenol_04262021_PIOV009NRAA-2306592.pdf.
[2] 2021. Ceramic Super-capacitor. https://www.ti.com/lit/ds/symlink/bq25570.pdf.
[3] 2021. Dynamic IR Scene Projector. https://www.acalbfi.com/be/Photonics/Uniform-sources-and-Camera-test-systems/Target-projectors/p/Dynamic-IR-Scene-Projectors--MIRAGE/0000001WFZ.
[4] 2021. Gel Filter Transparent Color Film Plastic Sheets. https://www.amazon.com/Pangda-Colored-Overlays-Correction-Transparent/dp/B07JPM33FC?th=1.
[5] 2021. Linx Ceramic Patch Antenna. https://www.mouser.com/pdfDocs/ant-915-cpa-ds.pdf.
[6] 2021. LTC6906 Linear Technology. https://www.analog.com/media/en/technical-documentation/data-sheets/6906fc.pdf.
[7] 2021. Oscillator. https://www.analog.com/en/products/ltc6906.html.
[8] 2021. Pansonite Mini Projector with High Brightness Support 1080P. https://www.amazon.com/dp/B07NPB66X3/ref=cm_sw_em_r_mt_dp_VHRFNC2ZCCY0CVT75H28?_encoding=UTF8&psc=1.
[9] 2021. RF Switch. https://www.analog.com/media/en/technical-documentation/data-sheets/ADG901_902.pdf.
[10] 2021. Silicon PIN Photodiode. https://www.vishay.com/docs/83471/tefd4300.pdf.
[11] 2021. VIVE Base Stations. https://www.vive.com/eu/accessory/base-station/.
[12] 2021. VIVE Trackers. https://www.vive.com/us/accessory/vive-tracker/.
[13] Roshan Ayyalasomayajula, Deepak Vasisht, and Dinesh Bharadia. 2018. BLoc: CSI-based accurate localization for BLE tags. In *Proceedings of the 14th International Conference on emerging Networking EXperiments and Technologies*. 126–138.
[14] Paul Bryant and Steve Solomon. 2007. Infrared scene projection: Virtual reality for IR sensor testing. *Photonics Spectra* 41, 4 (2007), 58–60.
[15] Liqiong Chang, Jie Xiong, Ju Wang, Xiaojiang Chen, Yu Wang, Zhanyong Tang, and Dingyi Fang. 2018. RF-copybook: A millimeter level calligraphy copybook based on commodity RFID. *Proceedings of the ACM on Interactive, Mobile, Wearable and Ubiquitous Technologies* 1, 4 (2018), 1–19.
[16] Li-Xuan Chuo, Zhihong Luo, Dennis Sylvester, David Blaauw, and Hun-Seok Kim. 2017. RF-Echo: A Non-Line-of-Sight Indoor Localization System Using a Low-Power Active RF Reflector ASIC Tag. In *Proceedings of the 23rd Annual International Conference on Mobile Computing and Networking (MobiCom '17)*. Association for Computing Machinery, New York, NY, USA, 222–234. https://doi.org/10.1145/3117811.3117840
[17] Joshua S Furtado, Hugh HT Liu, Gilbert Lai, Herve Lacheray, and Jason Desouza-Coelho. 2019. Comparative analysis of optitrack motion capture systems. In *Advances in Motion Sensing and Control for Robotic Applications*. Springer, 15–31.

[18] Francesco Guidi, Nicoló Decarli, Davide Dardari, Francesco Mani, and Raffaele D'Errico. 2018. Millimeter-wave beamsteering for passive RFID tag localization. *IEEE Journal of Radio Frequency Identification* 2, 1 (2018), 9–14.

[19] Robert K Harle and Andy Hopper. 2005. Deploying and evaluating a location-aware system. In *Proceedings of the 3rd international conference on Mobile systems, applications, and services*. 219–232.

[20] Cédric Honnet and Gonçalo Lopes. 2019. HiveTracker: 3D positioning for ubiquitous embedded systems. In *Adjunct Proceedings of the 2019 ACM International Joint Conference on Pervasive and Ubiquitous Computing and Proceedings of the 2019 ACM International Symposium on Wearable Computers*. 288–291.

[21] Chengkun Jiang, Yuan He, Songzhen Yang, Junchen Guo, and Yunhao Liu. 2019. 3D-OmniTrack: 3D tracking with COTS RFID systems. In *2019 18th ACM/IEEE International Conference on Information Processing in Sensor Networks (IPSN)*. IEEE, 25–36.

[22] Haojian Jin, Jingxian Wang, Zhijian Yang, Swarun Kumar, and Jason Hong. 2018. Rf-wear: Towards wearable everyday skeleton tracking using passive rfids. In *Proceedings of the 2018 ACM International Joint Conference and 2018 International Symposium on Pervasive and Ubiquitous Computing and Wearable Computers*. 369–372.

[23] Haojian Jin, Jingxian Wang, Zhijian Yang, Swarun Kumar, and Jason Hong. 2018. Wish: Towards a wireless shape-aware world using passive rfids. In *Proceedings of the 16th Annual International Conference on Mobile Systems, Applications, and Services*. 428–441.

[24] Paresh R Kamble, Avinash G Keskar, and Kishor M Bhurchandi. 2019. Ball tracking in sports: a survey. *Artificial Intelligence Review* 52, 3 (2019), 1655–1705.

[25] Manikanta Kotaru, Pengyu Zhang, and Sachin Katti. 2017. Localizing Low-Power Backscatter Tags Using Commodity WiFi. In *Proceedings of the 13th International Conference on Emerging Networking EXperiments and Technologies (CoNEXT '17)*. Association for Computing Machinery, New York, NY, USA, 251–262. https://doi.org/10.1145/3143361.3143379

[26] Ye-Sheng Kuo, Pat Pannuto, Ko-Jen Hsiao, and Prabal Dutta. 2014. Luxapose: Indoor Positioning with Mobile Phones and Visible Light. In *Proceedings of the 20th Annual International Conference on Mobile Computing and Networking (MobiCom '14)*. Association for Computing Machinery, New York, NY, USA, 447–458. https://doi.org/10.1145/2639108.2639109

[27] Elena Di Lascio, A. Varshney, T. Voigt, and C. Pérez-Penichet. 2016. LocaLight: a battery-free passive localization system using visible light: poster abstract. In *IPSN 2016*.

[28] Zhihong Luo, Qiping Zhang, Yunfei Ma, Manish Singh, and Fadel Adib. 2019. 3D Backscatter Localization for Fine-Grained Robotics. In *16th USENIX Symposium on Networked Systems Design and Implementation (NSDI 19)*. USENIX Association, Boston, MA, 765–782.

[29] Yunfei Ma, Xiaonan Hui, and Edwin C Kan. 2016. 3D real-time indoor localization via broadband nonlinear backscatter in passive devices with centimeter precision. In *Proceedings of the 22nd Annual International Conference on Mobile Computing and Networking*. 216–229.

[30] Yunfei Ma, Nicholas Selby, and Fadel Adib. 2017. Minding the Billions: Ultra-Wideband Localization for Deployed RFID Tags. In *Proceedings of the 23rd Annual International Conference on Mobile Computing and Networking (MobiCom '17)*. Association for Computing Machinery, New York, NY, USA, 248–260. https://doi.org/10.1145/3117811.3117833

[31] Verne H Mac Donald. 1979. Advanced mobile phone service: The cellular concept. *The bell system technical Journal* 58, 1 (1979), 15–41.

[32] Francisco Molina Martel, Juri Sidorenko, Christoph Bodensteiner, and Michael Arens. 2018. Augmented reality and UWB technology fusion: Localization of objects with head mounted displays. In *Proceedings of the 31st International Technical Meeting of the Satellite Division of The Institute of Navigation (ION GNSS+ 2018)*. 685–692.

[33] Rajalakshmi Nandakumar, Vikram Iyer, and Shyamnath Gollakota. 2018. 3d localization for sub-centimeter sized devices. In *Proceedings of the 16th ACM Conference on Embedded Networked Sensor Systems*. 108–119.

[34] Albert Ng, Michelle Annett, Paul Dietz, Anoop Gupta, and Walter F. Bischof. 2014. In the Blink of an Eye: Investigating Latency Perception during Stylus Interaction. In *Proceedings of the SIGCHI Conference on Human Factors in Computing Systems (CHI '14)*. Association for Computing Machinery, New York, NY, USA, 1103–1112. https://doi.org/10.1145/2556288.2557037

[35] Adrian KT Ng, Leith KY Chan, and Henry YK Lau. 2017. A low-cost lighthouse-based virtual reality head tracking system. In *2017 International Conference on 3D Immersion (IC3D)*. IEEE, 1–5.

[36] Edwin Olson. 2011. AprilTag: A robust and flexible visual fiducial system. In *2011 IEEE International Conference on Robotics and Automation*. IEEE, 3400–3407.

[37] Gopal Pingali, Agata Opalach, and Yves Jean. 2000. Ball tracking and virtual replays for innovative tennis broadcasts. In *Proceedings 15th International Conference on Pattern Recognition. ICPR-2000*, Vol. 4. IEEE, 152–156.

[38] Akarsh Prabhakara, Vaibhav Singh, Swarun Kumar, and Anthony Rowe. 2020. Osprey: A mmWave approach to tire wear sensing. In *Proceedings of the 18th International Conference on Mobile Systems, Applications, and Services*. 28–41.

[39] Nissanka B. Priyantha, Anit Chakraborty, and Hari Balakrishnan. 2000. The Cricket Location-Support System. In *Proceedings of the 6th Annual International Conference on Mobile Computing and Networking (MobiCom '00)*. Association for Computing Machinery, New York, NY, USA, 32–43. https://doi.org/10.1145/345910.345917

[40] Vaishnavi Ranganathan, Sidhant Gupta, Jonathan Lester, Joshua R. Smith, and Desney Tan. 2018. RF Bandaid: A Fully-Analog and Passive Wireless Interface for Wearable Sensors. *Proc. ACM Interact. Mob. Wearable Ubiquitous Technol.* 2, 2, Article 79, 21 pages. https://doi.org/10.1145/3214282

[41] Ramesh Raskar, Paul Beardsley, Jeroen van Baar, Yao Wang, Paul Dietz, Johnny Lee, Darren Leigh, and Thomas Willwacher. 2004. RFIG lamps: interacting with a self-describing world via photosensing wireless tags and projectors. In *ACM SIGGRAPH 2004 Papers*. 406–415.

[42] Ramesh Raskar, Hideaki Nii, Bert Dedecker, Yuki Hashimoto, Jay Summet, Dylan Moore, Yong Zhao, Jonathan Westhues, Paul Dietz, John Barnwell, et al. 2007. Prakash: lighting aware motion capture using photosensing markers and multiplexed illuminators. *ACM Transactions on Graphics (TOG)* 26, 3 (2007), 36–es.

[43] Alanson P Sample, Craig Macomber, Liang-Ting Jiang, and Joshua R Smith. 2012. Optical localization of passive UHF RFID tags with integrated LEDs. In *2012 IEEE International Conference on RFID (RFID)*. IEEE, 116–123.

[44] Ralph Schmidt. 1986. Multiple emitter location and signal parameter estimation. *IEEE transactions on antennas and propagation* 34, 3 (1986), 276–280.

[45] Chong Shao, Bashima Islam, and Shahriar Nirjon. 2018. Marble: Mobile augmented reality using a distributed ble beacon infrastructure. In *2018 IEEE/ACM Third International Conference on Internet-of-Things Design and Implementation (IoTDI)*. IEEE, 60–71.

[46] Sheng Shen, Mahanth Gowda, and Romit Roy Choudhury. 2018. Closing the gaps in inertial motion tracking. In *Proceedings of the 24th Annual International Conference on Mobile Computing and Networking*. 429–444.

[47] Soumitra P Sitole, Andrew K LaPre, and Frank C Sup. 2020. Application and Evaluation of Lighthouse Technology for Precision Motion Capture. *IEEE Sensors Journal* 20, 15 (2020), 8576–8585.

[48] Elahe Soltanaghaei, Akarsh Prabhakara, Artur Balanuta, Matthew Anderson, Jan M Rabaey, Swarun Kumar, and Anthony Rowe. 2021. Millimetro: mmWave retro-reflective tags for accurate, long range localization. In *Proceedings of the 27th Annual International Conference on Mobile Computing and Networking*. 69–82.

[49] Zhao Tian, Charles J. Carver, Qijia Shao, Monika Roznere, Alberto Quattrini Li, and Xia Zhou. 2020. PolarTag: Invisible Data with Light Polarization. In *Proceedings of the 21st International Workshop on Mobile Computing Systems and Applications (HotMobile '20)*. Association for Computing Machinery, New York, NY, USA, 74–79. https://doi.org/10.1145/3376897.3377854

[50] Deepak Vasisht, Guo Zhang, Omid Abari, Hsiao-Ming Lu, Jacob Flanz, and Dina Katabi. 2018. In-body backscatter communication and localization. In *Proceedings of the 2018 Conference of the ACM Special Interest Group on Data Communication*. 132–146.

[51] Jue Wang and Dina Katabi. 2013. Dude, where's my card? RFID positioning that works with multipath and non-line of sight. In *Proceedings of the ACM SIGCOMM 2013 conference on SIGCOMM*. 51–62.

[52] John Wang and Edwin Olson. 2016. AprilTag 2: Efficient and robust fiducial detection. In *2016 IEEE/RSJ International Conference on Intelligent Robots and Systems (IROS)*. IEEE, 4193–4198.

[53] Jingxian Wang, Chengfeng Pan, Haojian Jin, Vaibhav Singh, Yash Jain, Jason I Hong, Carmel Majidi, and Swarun Kumar. 2019. Rfid tattoo: A wireless platform for speech recognition. *Proceedings of the ACM on Interactive, Mobile, Wearable and Ubiquitous Technologies* 3, 4 (2019), 1–24.

[54] Jingxian Wang, Junbo Zhang, Ke Li, Chengfeng Pan, Carmel Majidi, and Swarun Kumar. 2021. Locating Everyday Objects using NFC Textiles. In *Proceedings of the 20th International Conference on Information Processing in Sensor Networks (co-located with CPS-IoT Week 2021)*. 15–30.

[55] Jingxian Wang, Junbo Zhang, Rajarshi Saha, Haojian Jin, and Swarun Kumar. 2019. Pushing the range limits of commercial passive rfids. In *16th {USENIX} Symposium on Networked Systems Design and Implementation ({NSDI} 19)*. 301–316.

[56] Teng Wei and Xinyu Zhang. 2015. mtrack: High-precision passive tracking using millimeter wave radios. In *Proceedings of the 21st Annual International Conference on Mobile Computing and Networking*. 117–129.

[57] Yu-Lin Wei, Chang-Jung Huang, Hsin-Mu Tsai, and Kate Ching-Ju Lin. 2017. Celli: Indoor positioning using polarized sweeping light beams. In *Proceedings of the 15th Annual International Conference on Mobile Systems, Applications, and Services*. 136–147.

[58] Owen M Williams. 1998. Dynamic infrared scene projection: a review. *Infrared Physics Technology* 39, 7 (1998), 473–486.

[59] Haijun Xia, Ricardo Jota, Benjamin McCanny, Zhe Yu, Clifton Forlines, Karan Singh, and Daniel Wigdor. 2014. Zero-Latency Tapping: Using Hover Information to Predict Touch Locations and Eliminate Touchdown Latency. In *Proceedings of the 27th Annual ACM Symposium on User Interface Software and Technology (UIST '14)*. Association for Computing Machinery, New York, NY, USA, 205–214.

[60] Fu Xiao, Zhongqin Wang, Ning Ye, Ruchuan Wang, and Xiang-Yang Li. 2017. One more tag enables fine-grained RFID localization and tracking. *IEEE/ACM Transactions on Networking* 26, 1 (2017), 161–174.

[61] Lei Yang, Yekui Chen, Xiang-Yang Li, Chaowei Xiao, Mo Li, and Yunhao Liu. 2014. Tagoram: Real-time tracking of mobile RFID tags to high precision using COTS devices. In *Proceedings of the 20th annual international conference on Mobile computing and networking*. 237–248.

[62] Faheem Zafari, Athanasios Gkelias, and Kin K Leung. 2019. A survey of indoor localization systems and technologies. *IEEE Communications Surveys & Tutorials* 21, 3 (2019), 2568–2599.

[63] Chi Zhang and Xinyu Zhang. 2016. LiTell: Robust indoor localization using unmodified light fixtures. In *Proceedings of the 22nd Annual International Conference on Mobile Computing and Networking*. 230–242.

[64] Chi Zhang and Xinyu Zhang. 2017. Pulsar: Towards ubiquitous visible light localization. In *Proceedings of the 23rd Annual International Conference on Mobile Computing and Networking*. 208–221.